UNIVERSITY OF BATH

Citation for published version:
Da Ros, S, Jones, M, Mattia, D, Pinto, J, Schwaab, M, Noronha, F, Kondrat, S, Clarke, T & Tayloar, S 2016, 'Ethanol to 1,3-butadiene conversion by using ZrZn-containing MgO-SiO_2 systems prepared by co-precipitation and effect of catalyst acidity modification', *ChemCatChem*, vol. 8, no. 14, pp. 2376-2386. https://doi.org/10.1002/cctc.201600331

DOI:
10.1002/cctc.201600331

Publication date:
2016

Document Version
Peer reviewed version

Link to publication

This is the peer reviewed version of the following article: Simoní DaRos Dr. Matthew D. Jones Dr. Davide Mattia Prof.Dr. Jose C. Pinto Dr. Marcio Schwaab Dr. Fabio B. Noronha Dr. Simon A. Kondrat Dr. Tomos C. Clarke Prof.Dr. Stuart H. Taylor (2016) Ethanol to 1,3Butadiene Conversion by using ZrZnContaining MgO/SiO2 Systems Prepared by Coprecipitation and Effect of Catalyst Acidity Modification. ChemCatChem, 8(14) which has been published in final form at 10.1002/cctc.201600331. This article may be used for non-commercial purposes in accordance with Wiley Terms and Conditions for Self-Archiving.

University of Bath

Alternative formats
If you require this document in an alternative format, please contact:
openaccess@bath.ac.uk

General rights
Copyright and moral rights for the publications made accessible in the public portal are retained by the authors and/or other copyright owners and it is a condition of accessing publications that users recognise and abide by the legal requirements associated with these rights.

Take down policy
If you believe that this document breaches copyright please contact us providing details, and we will remove access to the work immediately and investigate your claim.

Download date: 04. May. 2023

FULL PAPER

Ethanol to 1,3-butadiene conversion using ZrZn-containing MgO-SiO_2 systems prepared by co-precipitation and effect of catalyst acidity modification

Simoní Da Ros, [a,b] Matthew D. Jones, *[b] Davide Mattia, [c] Jose C. Pinto,*[a] Marcio Schwaab, [d] Fabio B. Noronha, [e] Simon A. Kondrat, [f] Tomos C. Clarke, [f] and Stuart H. Taylor [f]

Abstract: The conversion of ethanol to 1,3-butadiene (1,3-BD) has been investigated over ZrO_2 and ZnO containing magnesia silica oxides prepared by co-precipitation method at different Mg-to-Si molar ratios. The effect of reaction temperature and ethanol flow rate was investigated. The catalyst acidity was modified through the addition of alkali metals (Na, K and Li) to the final materials. Catalysts were characterised by nitrogen physisorption analysis, X-ray diffraction, scanning electron microscopy with energy dispersive X-ray, temperature programmed desorption of ammonia, infrared spectroscopy and $^{29}Si/(^{7}Li)$ NMR spectroscopy. The catalytic results showed that the controlled reduction of catalyst acidity allows suppressing of ethanol dehydration, whilst increasing 1,3-BD selectivity. The best catalytic performance achieved 72 mol % for the combined 1,3-BD and acetaldehyde selectivity.

Introduction

1,3-butadiene (1,3-BD) is an important starting material used as a monomer for the production of a variety of synthetic polymers.[1] The polymerisation of 1,3-BD with itself and with other olefin monomers represents its largest commercial use, examples include the production of styrene-butadiene-rubber (SBR), polybutadiene (PB), styrene-butadiene latex (SBL), acrylonitrile-butadiene-styrene (ABS), adiponitrile, nitrile rubber (NBR), chloroprene, styrene-butadiene block copolymers (SBS and SEBS).[2] 1,3-BD is currently produced from naphtha steam crackers, as a co-product of ethene manufacturing.[3,4] Besides environmental concerns as a result of the use of petroleum-derived hydrocarbons, the need for a new route to 1,3-BD is further exacerbated due to the possible future shortfall in supply due to the changes of feedstock from naphtha to ethane in the U.S.[5,6] The catalytic conversion of ethanol into 1,3-BD is an attractive alternative, due to the availability of bioethanol which is expected to significantly increase over the next few years from fermentation of sugar rich waste materials (second generation bioethanol).[1,5,7,8] For example in Brazil alone, 23.4 billion litres of bioethanol were produced in 2014.[9]

The route most widely accepted to account for 1,3-BD production from ethanol involves five consecutive reactions.[10-16] Initially, ethanol is dehydrogenated to acetaldehyde. Then, 3-hydroxybutanal is formed from acetaldehyde self-aldolisation. Next, 3-hydroxybutanal dehydrates to crotonaldehyde, which is reduced (Meerwein-Ponndorf-Verley (MPV) reduction) with ethanol to produce crotyl alcohol and acetaldehyde. Finally, crotyl alcohol is dehydrated to afford 1,3-BD. This mechanism was initially suggested and experimentally supported by Quattlebaum *et al*.,[17] who verified that higher 1,3-BD yields were achieved when crotonaldehyde and ethanol were used compared to a feed comprising acetaldehyde and ethanol, with either a SiO_2 based system or Ta_2O_5/SiO_2 catalyst. With the latter catalyst, the authors also observed that a feed comprising of only acetaldehyde was converted into crotonaldehyde, which was not observed in significant quantities when ethanol and acetaldehyde were passed over the catalyst. This suggests that crotonaldehyde was rapidly converted into crotyl alcohol (presumably by an MPV process) and subsequently to 1,3-BD. However, some reports have recently ruled out the aldol condensation as the main path, suggesting instead that crotyl alcohol is produced through the reaction between an activated form of ethanol and acetaldehyde.[18,19]

Due to the specific features of the catalyst that are required for this cascade reaction, materials with multifunctional properties have been studied, especially MgO-SiO_2 systems.[2,5] This is related to the fact that Mg-O pairs might act as Lewis acid-Brønsted basic sites and the silanol functionality as a Brønsted acid which are necessary for ethanol dehydrogenation,[20] acetaldehyde condensation,[21] crotonaldehyde reduction and the further crotyl alcohol dehydration to 1,3-BD. However, due to the presence of acid sites in these systems, ethanol dehydration to ethene and diethyl ether are significant competitive reactions. Efforts have been dedicated to the design of catalysts able to

[a] *S. Da Ros, Dr. J. C. Pinto*
Programa de Engenharia Química/COPPE
Universidade Federal do Rio de Janeiro
Cidade Universitária-CP: 68502, 21941-972, Rio de Janeiro (Brazil)
E-mail: pinto@peq.coppe.ufrj.br
[b] *Dr. M. D. Jones*
Department of Chemistry
University of Bath
Claverton Down, Bath BA2 7AY (UK)
E-mail: mj205@bath.ac.uk
[c] *Dr. D. Mattia*
Department of Chemical Engineering
University of Bath
Claverton Down, Bath BA2 7AY (UK)
[d] *Dr. M. Schwaab*
Departamento de Engenharia Química
Universidade Federal do Rio Grande do Sul, 90040040, Porto Alegre (Brazil)
[e] *Dr. F. B. Noronha*
Catalysis Division
National Institute of Technology
Av. Venezuela 82, 20081-312, Rio de Janeiro (Brazil)
[f] *S. A. Kondrat, Dr. T. C. Clarke, Dr. S. H. Taylor*
School of Chemistry, Cardiff Catalysis Inst.
Cardiff University
CF10 3AT, Cardiff (Wales)

Supporting information for this article is given via a link at the end of the document.

WILEY-VCH

suppress these undesirable parallel reactions. For instance, the addition of metals and/or metal oxides based on Cu, Zr, Zn and Ag to the MgO-SiO_2 system has been shown to be beneficial to 1,3-BD yield.[13,21-23,28] In particular, a synergic effect between ZrO_2 and ZnO has been demonstrated.[12,23] ZnO may support ethanol dehydrogenation and ZrO_2 is expected to assist aldol condensation and crotonaldehyde reduction.[12,14,23,28-30] Conversely, besides catalyst composition, the catalyst preparation method is of paramount importance for 1,3-BD formation, since different acid-basic features may be obtained depending on synthesis conditions.[18,22,23,31] Due to this, it has been reported different optimum Mg-to-Si molar ratios for 1,3-BD formation, depending on the synthesis procedure employed.[13,18,23]

Among the catalyst preparation procedures, different methods have been investigated such as physical mixtures of MgO and SiO_2,[11,13] wet-kneading,[10-13,22,23] sol-gel,[18,24] impregnation[13] and co-precipitation.[22,25,26] Whereas it has been proven that a physical mixture between precursor oxides is not suitable for 1,3-BD formation, since resultant catalysts show similar features to single MgO and SiO_2 phases, wet-kneading methods have been the most widely discussed in the literature with less attention being dedicated to sol-gel and co-precipitation methods.[5]

In the wet-kneading preparation procedure, MgO and SiO_2 are usually mixed at the desired molar ratio in the presence of water, dried and calcined. Besides the specific features of the MgO and SiO_2 precursors employed and their molar ratio, the amount of water, time, ageing temperature, drying and calcination procedure represent some of the preparation steps that might alter the catalysts behaviour.[5] As observed by EDX and TEM analyses, materials prepared by wet-kneading are usually inhomogeneous in their composition and morphology.[11,22,27] They are generally constituted by ¨islands¨ of MgO and SiO_2, and a limited amount of amorphous magnesia hydrosilicate phase.[22,27] These unique characteristics are described as the key factor for the conversion of ethanol into 1,3-BD, since an intrinsic basic-acid sites distribution is obtained on these materials.[22,27]

Using a sol-gel method, Ochoa *et al*.[18] observed that the Mg:Si molar ratio affected the number, strength and distribution of basic-acid sites, the surface area and the crystalline structure of the catalysts, impacting on product distribution. A comparison between wet-kneading and a co-precipitation method, at the same Mg:Si ratio, has pointed to the former as more suitable for ethanol conversion into 1,3-BD.[22,27] However, the co-precipitation method may be an efficient preparation procedure in order to produce catalysts with homogeneous properties throughout their surface, therefore increasing the potential of controlling the physical and chemical properties of the catalyst and facilitating the determination of structure-activity-relationships. Despite that, a rigorous study using the co-precipitation method has not been reported.

Herein, we report for the first time an extensive investigation using the co-precipitation method for the synthesis of magnesium silica oxide catalysts with different Mg-to-Si (Mg:Si) molar ratios for ethanol conversion into 1,3-BD. The materials were used as supports for ZnO and ZrO_2 doping and the Mg:Si molar ratio effect of materials containing ZrO_2 and ZnO was also evaluated. The effect of reaction temperature and ethanol flow rate was also studied. In particular, the ethanol flow rate was investigated in order to assess catalyst performance regarding 1,3-BD productivity (in $g_{BD}/g_{cat}.h$), a variable usually neglected [18,22,32,33] that is important for industrial applications. Since it is well-known that the acidic-basic features play a key role for this process, we have modified the catalyst acidity through the addition alkali metals (Na, K and Li) to the final materials. The catalyst preparation method was further optimized by the modification of the number of calcination steps. As a result, it is shown that the co-precipitation method is suitable to prepare MgO-SiO_2 systems that, after ZrO_2 and ZnO addition, produce 1,3-BD productivities as high as the obtained using expensive Ag containing systems.[2,14] Besides this, the catalyst acidity modification through the alkali metal doping was successful for the suppression of ethanol dehydration , allowing the combined 1,3-BD and acetaldehyde selectivity to be increased up to 72 %. Catalysts were characterised by nitrogen physisorption, X-ray diffraction, scanning electron microscopy with energy dispersive X-ray, temperature programmed desorption of ammonia, infrared spectroscopy and $^{29}Si/(^{7}Li)$ NMR spectroscopy.

Results and Discussion

The effect of the Mg:Si molar ratio

Magnesium silica oxide catalysts prepared at different Mg:Si molar ratios were evaluated at 325 °C, using an ethanol weight hourly space velocity (WHSV) of 0.62 h^{-1}. At this condition, ethanol conversion was typically lower than 20 %, allowing a clear observation of the different catalytic properties among the catalysts samples.

Figure 1 shows the selectivity profile of the main carbon containing products, obtained after 3 h of time on stream (TOS), as a function of the Mg:Si molar ratio for (a) MgO-SiO_2 systems and (b) MgO-SiO_2 systems containing a fixed amount of ZrO_2 and ZnO, which has previously shown to be optimum for SiO_2 and acts as a comparison to our previous work.[12,23] Profiles observed for ethene, diethyl ether (DEE) and acetaldehyde (AcH) show the same general trend as a function of the Mg:Si molar ratio. Whereas ethene and DEE selectivities decreased as the Mg:Si molar ratio was increased, AcH selectivity showed a sharp increase, from less than 10 % with the 1:1 species to over 40 % with higher amounts of MgO. The decrease in the ethanol dehydration along with the increase in the ethanol dehydrogenation as the Mg:Si molar ratio was increased is in agreement with a reduction in the catalyst acidity, as expected when the Mg:Si increases.[10,18]

On the other hand, interestingly, the effect of the Mg:Si molar ratio on 1,3-BD selectivity was different between MgO-SiO_2 systems and MgO-SiO_2 systems containing ZrO_2 and ZnO. While a smooth rise in 1,3-BD selectivity was verified as the Mg:Si molar ratio increased for pure MgO-SiO_2 samples, Figure 1 (a), the same trend was not observed for

catalysts containing ZrO_2 and ZnO, Figure 1(b). Instead, a maximum in the 1,3-BD selectivity was obtained for the catalyst with the Mg:Si molar ratio equal to one.

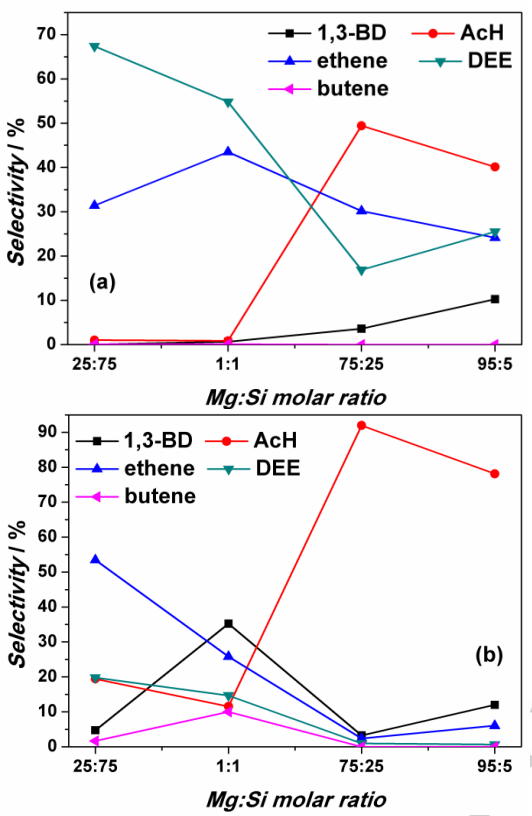

Figure 1. Mg:Si molar ratio effect on main carbon containing reaction products for (a) MgO-SiO_2 systems and (b) MgO-SiO_2 systems containing ZrO_2 and ZnO (T = 325 ºC, TOS = 3 h, WHSV = 0.62 h^{-1}, contact time = 4 s).

We have previously studied the effect of the Mg:Si molar ratio for Zn(II) and Zr(IV) containing MgO-SiO_2 systems, using the wet-kneading method in the MgO-SiO_2 preparation.[12] In line with results presented in Figure 1, MgO-SiO_2 systems prepared by the wet-kneading method have shown a different 1,3-BD selectivity behaviour upon the addition of ZrO_2:ZnO to the catalyst. However, while a maximum in the 1,3-BD selectivity was observed at the Mg:Si molar ratio equal to 3:1 for the pure MgO-SiO_2 systems, an increase in 1,3-BD selectivity was observed as the Mg:Si molar ratio was increased for the systems prepared by incipient wetness.[12] These results are in contrast with those reported here, in Figure 1, emphasising that the co-precipitation preparation procedure has dramatically changed the physicochemical properties of the catalyst compared to the wet-kneading procedure.

Regarding textural properties, samples with higher Mg:Si molar ratio showed lower surface areas compared to the 1:1 and 25:75 ratios, which may indicate the formation of MgO particles in the pores of the samples, Table S1 in the supporting information.[13,23] Diffraction patterns indicated samples with amorphous features, the MgO periclase phase being observed only in the MgO-SiO_2-(95:5) sample (peaks at Bragg angles of 37.0º, 43.0º, 62.4º),[2] Figure S1. In particular, the ZrZn/MgO-SiO_2-1 system presented broad peaks (at 25-30°, 33-39° and 58-62°) characteristic of magnesium silicate hydrates.[34,35] Since samples containing ZrO_2 and ZnO have shown similar pXRD patterns compared to the initial MgO-SiO_2 support, ZrO_2 and ZnO should be dispersed into the -Mg-O-Si- network or their small loading was undetectable by pXRD. These results highlight the effect of preparation method on catalyst properties, since MgO phase was observed even for Mg:Si molar ratio equal to 1, using a sol-gel technique.[18]

A clear modification of silicon environments as a function of the Mg:Si molar ratio was suggested by $^{29}Si\{^1H\}$ CP MAS NMR experiments, Figure S2. Catalysts with higher amount of MgO, MgO-SiO_2-(95:5) and MgO-SiO_2-(75:25) samples, presented a single resonance with maxima around -71 ppm, indicating a high concentration of Q^1 species. Conversely, as the Mg:Si molar ratio was decreased, MgO-SiO_2-(1:1) and MgO-SiO_2-(25:75) samples, resonances maxima were shifted down field, to ca. -87 and -94 ppm, indicating an increase in Q^2 and Q^3 species [2,34,36]. In comparison with the wet-kneading method,[23] Q^2 and Q^3 species were observed at the Mg:Si molar ratio equal to 75:25, and Q^2, Q^3 and Q^4 species were observed at the Mg:Si molar ratio equal to 1. Thus, the co-precipitation method used in this work seems to be more efficient in the formation of Mg-O-Si linkages. These results are in agreement with a general uniform distribution of elements inside catalyst particles as verified for the ZrZn/MgO-SiO_2-1 sample by scanning electron microscopy with energy dispersive X-ray, Figure S3. Even though a residual amount of Na was observed, from catalyst preparation, as it will be more detailed in the catalyst characterisation section, these Na traces did not significantly affect catalyst activity.

Since the synergistic effect of ZrO_2 and ZnO on the MgO-SiO_2 system was more beneficial to 1,3-BD formation at the Mg:Si molar equal to one, this catalytic system, labelled as ZrZn/MgO-SiO_2-1, was selected for further investigation.

Reaction temperature and WHSV effect

Initially, reaction temperature and the WHSV effect were investigated in order to evaluate catalyst performance and afford more insights to the kinetic mechanism. Mass transfer limitations were excluded by the apparent activation energy estimation,[37] Fig. S4.

The effect of reaction temperature and WHSV on ethanol dehydration products is shown in Figure 2. It should be noted that, in this work, higher WHSV conditions correspond to higher ethanol molar fraction in gas phase and lower contact times.

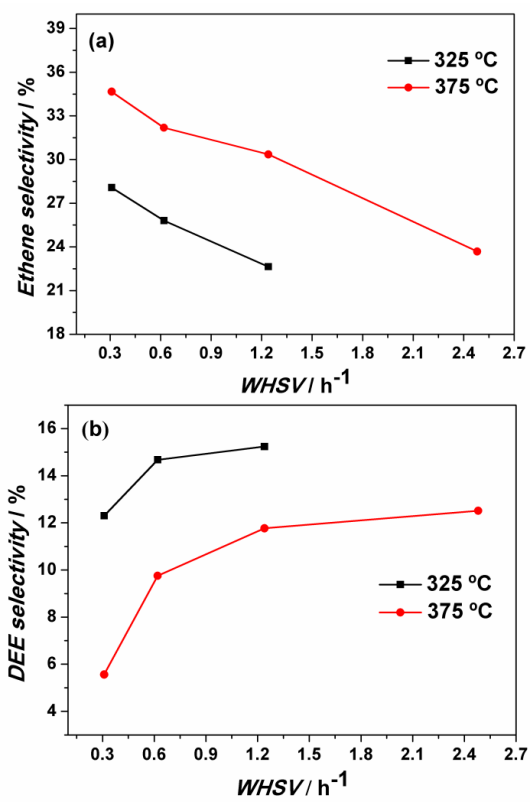

Figure 2. WHSV and reaction temperature effect on (a) ethene and (b) DEE selectivities (ZrZn/MgO-SiO_2-1, TOS = 3 h).

As expected, an increase in reaction temperature increased ethene selectivity, Figure 2(a), and decreased DEE selectivity, Figure 2(b), ethanol dehydration to ethene is endothermic and to DEE is exothermic.[7,38] Even though the mechanism of DEE formation is still discussed in the literature, for instance, regarding whether it involves acid-base pairs,[39,40] Brønsted acid sites and/or Lewis acid sites,[40] it is understood that DEE formation should involve the reaction of the two nearest chemisorbed ethanol moieties.[41] On the other hand, ethene formation should occur through a concerted mechanism, where the methyl hydrogen of the ethoxide species, chemisorbed on a Lewis[41] or Brønsted acid site,[42] is abstracted by the adjacent Brønsted basic site. Indeed, using an alumina catalyst, Arai *et al*.[41] verified a rise in DEE formation as the concentration of surface ethoxide was increased, while ethene formation was suppressed. Therefore, the effect of WHSV on ethene and DEE selectivities observed in this work suggests an increase in the concentration of chemisorbed ethanol species on the catalyst surface with a concurrent increase in WHSV, since higher ethanol molar fractions were fed at higher WHSV conditions.

Figure 3 shows the effect of reaction temperature and WHSV on AcH and 1,3-BD selectivities. AcH has shown a selectivity increase for both reaction temperatures as WHSV was raised, Figure 3(a). Since ethanol dehydrogenation to AcH should involve Brønsted basic sites and Lewis acid sites,[20,43] verified tendencies suggest a high concentration of active sites for ethanol dehydrogenation on the catalyst surface.

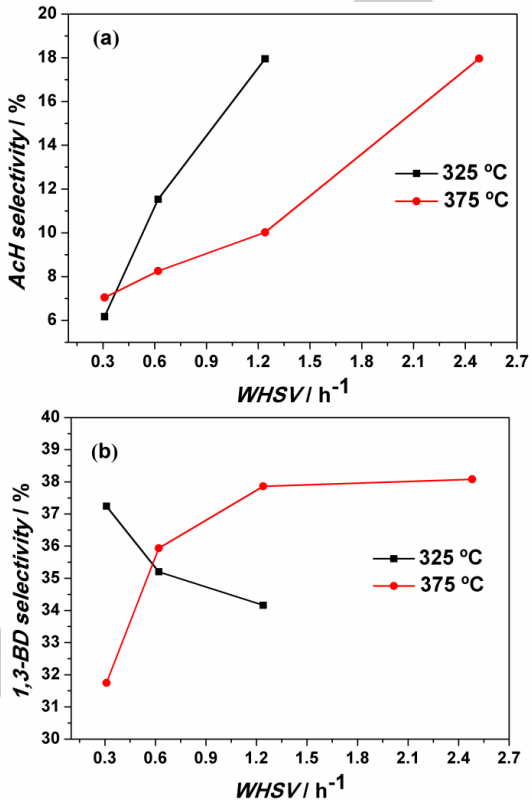

Figure 3. WHSV and reaction temperature effect on (a) AcH and (b) 1,3-BD selectivities (ZrZn/MgO-SiO_2-1, TOS = 3 h).

The further AcH transformation involves 3-hydroxybutanal formation and its subsequent dehydration to crotonaldehyde.[5,12] Whereas the aldol coupling is an endergonic reaction in the temperature range studied, which becomes more endergonic as reaction temperature increases,[5] 3-hydroxybutanal dehydration to crotonaldehyde is favourable in this temperature range and becomes more favourable as the temperature increases.

Thus, since ethanol dehydrogenation to AcH is favoured thermodynamically as the reaction temperature increases,[5] an excess of acetaldehyde in the system might contribute to further AcH condensation, explaining its lower selectivities at 375 °C.

1,3-BD selectivity behaviour has presented different tendencies as a function of reaction temperature and WHSV, Figure 3(b). While at the higher temperature the increase of 1,3-BD selectivity as WHSV increased might be related to an excess of AcH in the system, at the lower temperature, contact time appears to be affecting 1,3-BD formation more dramatically. This same effect of residence time was observed by Sushkevich *et al*.[14], who evaluated the WHSV effect using an Ag/ZrO_2/SiO_2 system at 320 °C. Besides,

additional experiments varying the WHSV at 375ºC and using the same ethanol molar fraction (the amount of catalyst remained constant and the gas flow and ethanol feed rate were both varied), indicated the same general tendency observed at 325 ºC, Figure S4(c). This implies that the extra ethanol present in the higher WHSV processes facilitates the full conversion to 1,3-BD, as observed previously.[12]

Butene selectivity (1-butene, *cis*- and *trans*-2-butene) decreased smoothly as the WHSV was increased at both reaction temperatures, Figure 4. The formation of butene from ethanol is thought to occur through deoxygenation of butanal produced from crotyl alcohol isomerisation.[5] Other studies suggest butene as a butanol dehydration product, butanol being produced from the hydrogenation of butanal, which in turn, might be obtained from the hydrogenation of the C=C double bond of crotonaldehyde.[16,25] However, no traces of butanal, or butanol were observed in this work and butene may be a product of 1,3-BD hydrogenation. Thus, the reduction in butene selectivity with WHSV can be explained by a reduction of contact time of 1,3-BD in the reactor.

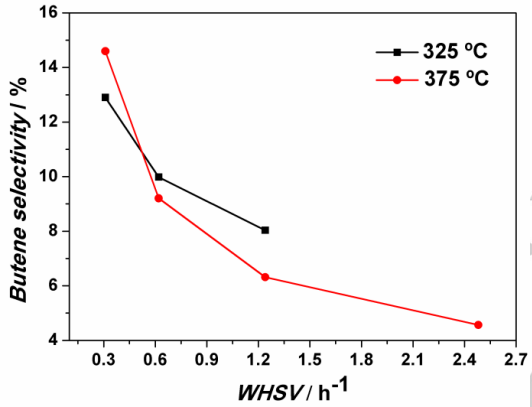

Figure 4. WHSV and reaction temperature effect on butene selectivity (ZrZn/MgO-SiO_2-1, TOS = 3 h).

Other minor products observed were ethane, acetone, propene and propane, their combined selectivities have not achieved more than 7 % in all experiments. Traces of ethyl acetate, C5 (pentadienes and its isomers) and C6 (hexadienes) compounds were also identified in the output stream.

Regarding ethanol conversion, an increase was observed as reaction temperature increased, whereas an ethanol conversion drop was observed as WHSV was raised, Figure 5. The higher WHSV increases the ethanol molar fraction in the gas stream, at the same time shortening contact time, factors that might help to explain the reduced conversion.

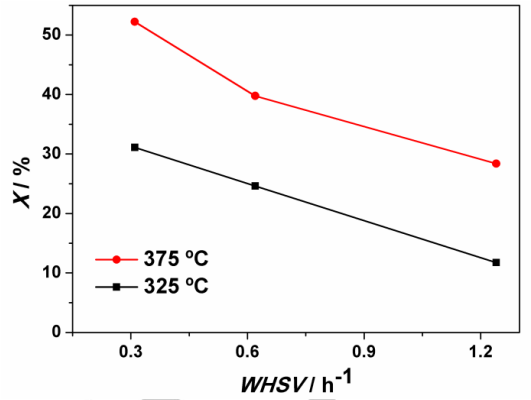

Figure 5. WHSV and reaction temperature effect on ethanol conversion (ZrZn/MgO-SiO_2-1, TOS = 3 h).

Figure 6 shows the effect of reaction temperature and WHSV on the yield of the main carbon containing reaction products. Firstly, it is worth noting that the ethanol conversion increase resulted from the temperature rise has boosted 1,3-BD yield from 9-16 % at 325 °C to 27-30 % at 375 °C, within the same range of WHSV between 0.3 and 1.2 h^{-1}.

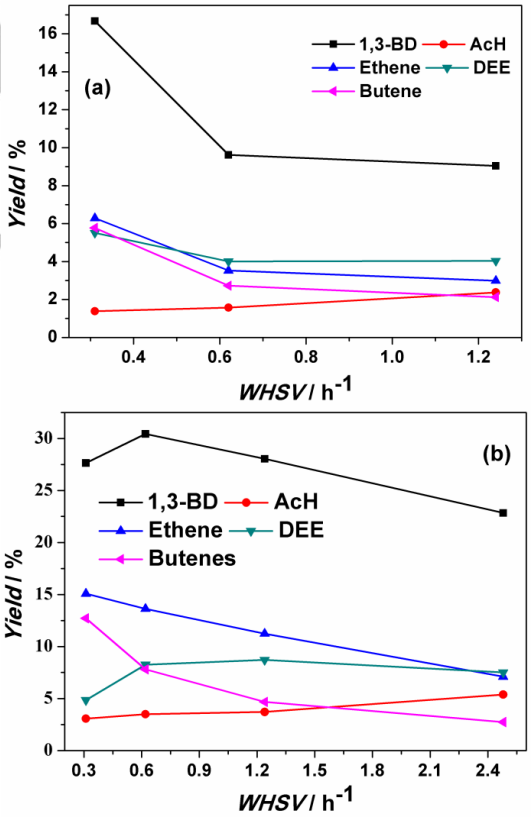

Figure 6. Effect of WHSV on yield of the main carbon containing products at (a) 325 °C and (b) 375 °C. (ZrZn/MgO-SiO_2-1, TOS = 3 h).

Moreover, even though the increase in WHSV has reduced ethanol conversion, Figure 5, 1,3-BD yield has only reduced

slightly. Thus, a linear increase on BD productivity (in g_{BD}/g_{cat}·h) was obtained with WHSV, Figure 7.

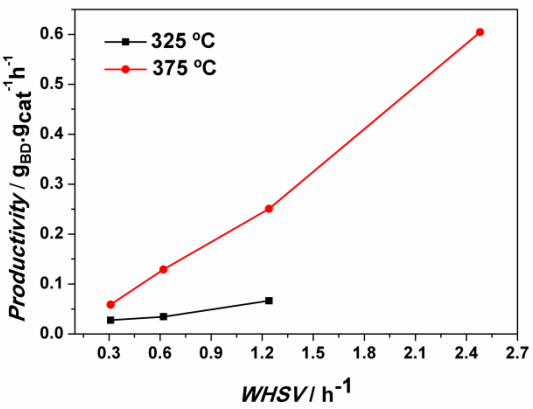

Figure 7. Effect of WHSV and reaction temperature on 1,3-BD productivity (g_{BD}/g_{cat}·h) on ZrZn/MgO-SiO_2-1 catalyst (TOS = 3 h).

As discussed by Makshina *et al.*,[13] catalytic data is usually reported at low ethanol concentrations and 1,3-BD productivities are usually too low to be industrially relevant. 1,3-BD productivity values achieved in this work suggest that the ZrZn/MgO-SiO_2-1 material prepared by co-precipitation is a promising catalyst for 1,3-BD production, as it presents high productivity with reasonable 1,3-BD selectivity, when compared to other catalytic systems.[13,30] For instance, Janssens *et al.*[2] has reported productivity equal to 0.15 g_{BD}/g_{cat}·h over a catalyst based on Ag/MgO-SiO_2, at 400 ºC and WHSV = 1.2 h^{-1}. Using a lower temperature (320 ºC), but much higher WHSV (10.3 h^{-1}), Sushchevich *et al.*[14] observed 0.23 g_{BD}/g_{cat}·h over a Ag/ZrO_2/SiO_2 system.

Based on these results, we conclude that our ZrZn/MgO-SiO_2-1 catalyst has shown suitable performance for ethanol to 1,3-BD conversion. However, ethanol dehydration was present in significant quantities and, thus, we aimed to modify the acidic features of this system through the addition of the alkali metals Na, K and Li.

Catalyst acidity modification

The effect of added Na_2O content on selectivity for the main carbon containing products is shown in Figure 8(a). The increase in Na_2O content decreased the selectivities to ethene and diethyl ether, while increasing the selectivities to 1,3-BD and AcH. Conversely, no significant change was observed to butene selectivity, which fluctuated around 10 %.

A positive linear relation was verified when 1,3-BD and AcH selectivities were considered as a function of Na_2O content, Figure 8(b), achieving 66 % to the combined 1,3-BD and AcH selectivities for the sample with the highest Na content. Also, a negative linear relation was obtained when ethene and DEE selectivities were considered as a function of catalyst Na_2O content, Figure 8(b).

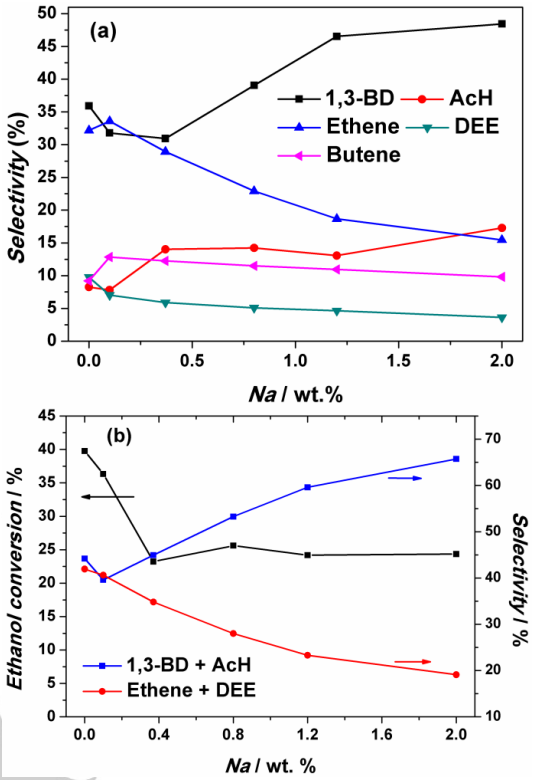

Figure 8. (a) Effect of catalyst Na content on the selectivity of the main carbonaceous products and (b) selectivities comparison with ethanol conversion. (T = 375 °C, WHSV = 0.62 h^{-1}, TOS = 3 h).

Moreover, a reduction in ethanol conversion was observed as a function of Na content, Figure 8(b), resulting in lower 1,3-BD yields and productivities, Table 1, entries 1-4. These tendencies were confirmed using a lower WHSV equal to 0.3 h^{-1}, entries 5-7, Table 1. However, it should be emphasised that avoiding ethanol dehydration is the most important step to attain high 1,3-BD yields, since ethene is the most thermodynamically stable product.[5] The thermodynamics of the reaction mixture in the case where ethanol dehydration occurs together with ethanol to 1,3-BD conversion was discussed by Makshina et al.,[5] who have shown that the thermodynamic yield of 1,3-BD is considerably lower when ethanol dehydration is present.

The suppression of acid sites through Na doping was recently studied on $Zn_xZr_yO_z$ mixed metal oxides in the ethanol to 1,3-BD conversion.[30] An increase in the AcH and 1,3-BD selectivity and a decrease in ethene selectivity were observed for Na_2O containing samples. The catalytic results were rationalised through a reduction in the number of strong acid sites due to Na doping, which was verified by temperature programmed desorption of ammonia (NH_3-TPD).

.

Table 1. Catalytic results for 3 h of time on stream and reaction temperature equal to 375 °C.

Entry	Catalyst	WHSV	X (%)	Selectivity (mol%)					1,3-BD yield[d] (mol%)	1,3-BD productivity ($g_{BD}/g_{cat}\cdot h$)
				1,3-BD	AcH	Ethene	DEE	Butene		
1	ZrZn/MgO-SiO_2-1	0.62	40	35.9	8.3	32.2	9.8	9.2	30.4	0.13
2	0.8-Na/ZrZn/MgO-SiO_2-1	0.62	26	39.1	14.2	22.9	5.1	11.5	18.1	0.08
3	1.2-Na/ZrZn/MgO-SiO_2-1	0.62	24	46.5	13.1	18.7	4.6	10.9	17.3	0.07
4	2-Na/ZrZn/MgO-SiO_2-1	0.62	24	48.5	17.3	15.5	3.6	9.8	13.7	0.06
5	ZrZn/MgO-SiO_2-1	0.31	52	31.8	7.0	34.7	5.6	14.6	27.6	0.06
6	1.2-Na/ZrZn/MgO-SiO_2-1	0.31	35	49.3	11.8	16.3	4.4	12.4	25.4	0.05
7	2-Na/ZrZn/MgO-SiO_2-1	0.31	36	50.6	16.9	13.8	3.4	9.9	17.4	0.03
8	Water/ZrZn/MgO-SiO_2-1	0.62	46	32.5	6.6	34.9	10.4	10.6	26.8	0.11
9[a]	1.2-Na/ZrZn/MgO-SiO_2-1	0.62	28	52.2	20.0	10.5	2.7	10.2	19.6	0.09
10[b]	ZrZn/MgO-SiO_2-1	0.62	32[c]	44.6	8.2	24.2	6.6	10.8	41.4	0.17
11[a,b]	1.2-Na/ZrZn/MgO-SiO_2-1	0.62	6.9[c]	44.7	34.1	5.8	1.2	9.9	25.4	0.10
12	1.2-K/ZrZn/MgO-SiO_2-1	0.62	22	51.6	13.7	17.4	5.2	7.5	21.1	0.09
13	1.2-Li/ZrZn/MgO-SiO_2-1	0.62	18	44.3	20.5	16.2	4.4	8.7	11.4	0.05
14[d]	ZrZn/MgO-SiO_2-1	0.62	44	26.2	6.3	43.6	12.7	7.5	24.6	0.11
15[a,e]	1.2-Na/ZrZn/MgO-SiO_2-1	0.62	19	49.5	22.8	11.3	3.2	9.0	22.2	0.10
16[a,e]	1.2-K/ZrZn/MgO-SiO_2-1	0.62	26	55.1	17.1	12.2	3.5	7.9	27.1	0.12
17[a,e]	1.2-Li/ZrZn/MgO-SiO_2-1	0.62	19	47.7	17.0	13.4	2.6	13.7	15.9	0.07
18[a,e]*	1.2-K/ZrZn/MgO-SiO_2-1	0.31*	44	57.8	12.9	10.3	2.5	10.3	37.2	0.07
19[a,e]*	1.2-K/ZrZn/MgO-SiO_2-1	0.62*	35	55.9	19.2	10.2	2.78	7.5	20.1	0.09
20[a,e]*	1.2-K/ZrZn/MgO-SiO_2-1	1.24*	26	44.6	30.9	7.5	2.36	5.0	13.1	0.12

[a] No calcination after alkali metal doping. [b] Acetaldehyde in the feed (8:2 ethanol to AcH feed ratio). [c] Acetaldehyde conversion was not calculated. [d] Calculated with Equation 3. [e] No calcination before Zr and Zn addition. *Ethanol molar fraction was kept equal to 0.4.

In this work, catalysts acidity of samples was investigated through ammonia adsorption followed by TPD experiments and IR measurements. Gases released during TPD experiments were monitored by MS, Figure S5. A dramatic reduction in the *m/z* signal attributed to NH_3, from the ZrZn/MgO-SiO_2-1 system to samples impregnated with sodium, was verified, indicating a large reduction in the number of acidic sites. A minor reduction in the number of acidic sites as the quantity of sodium was increased in the samples was also indicated by NH_3-TPD experiments, Table S2. Furthermore, sodium containing samples presented peaks with maximum intensity at temperature around 380 ºC, Figure S5(b), whilst the ZrZn/MgO-SiO_2-1 system exhibited peak maximum intensity around 520 ºC. Therefore, the addition of sodium resulted in a reduction on the concentration and strength of the acid sites.

IR measurements after NH_3 adsorption supported NH_3-TPD conclusions, presenting a clear reduction in the NH_3 stretching intensity as Na content was increased in the samples, Figure S6. In particular, a weaker NH_3 signal was observed for the precursor MgO-SiO_2-1 material, indicating that the ZrO_2 and ZnO addition increased the acidity from the MgO-SiO_2-1 to the ZrZn/MgO-SiO_2-1 system. Thus, the sodium addition should have deactivated Lewis acid sites associated to ZrO_2 and ZnO, as it will be more discussed later, contributing to the reduction of the ethanol dehydrated fraction and ethanol conversion.

As expected, however, besides acidity, the sodium addition modified samples textural properties as well. While no significant change on pore structure was indicated by N_2 adsorption-desorption isotherms, Figure S7, surface area reduced with Na content, Table S3, probably due to Na_2O particles formation in the catalyst pores.[13,23] Thus, the ethanol conversion reduction should be associated, mainly, to the deactivation of acid sites and to the smaller access to active sites as a result of surface area reduction.

The Na_2O effect on the catalytic properties was confirmed by an additional experiment where the process of Na addition was imitated using only water, entry 8, Table 1. The catalytic performance was similar to the obtained for the ZrZn/MgO-SiO_2-1 (entry 1, Table 1) system. Thus, the additional calcination step involved in the Na addition process, which is illustrated in the Figure S8 as *Calcination 3*, did not appear to have affected catalyst activity, and therefore, the effect of removal of this calcination step was investigated, entry 9, Table 1. A slight increase in the 1,3-BD selectivity, yield and productivity (compare entries 3 and 9) was obtained. However, there is a difference in the surface

area, (219 vs 333 m²/g) of the two materials, which may contribute to the difference in performance.

In an attempt to further improve the catalytic data, the effect of acetaldehyde in the feed was evaluated using an ethanol-to-acetaldehyde feed ratio equal to 8:2, since this condition has resulted in better catalytic performances in previous literature.[12] Catalytic data is shown in Table 1 (entries 10-11). As expected, the addition of AcH in the feed increased the amount of 1,3-BD produced (compare yields and productivities between entries 1 and 10, and between entries 9 and 11, Table 1). Moreover, ethanol dehydration to ethene and DEE was further suppressed upon AcH addition, this suppression being more pronounced for the catalyst containing Na_2O.

The acidity modification of the ZrZn/MgO-SiO_2-1 system was also investigated using two other alkali metals, K and Li, entries 12 and 13, Table 1. Both systems were effective in the suppression of ethanol dehydration, presenting lower selectivities to ethene and DEE compared to the starting ZrZn/MgO-SiO_2-1 material. A similar catalytic performance was observed between samples doped with Na and K (compare entry 3 and 12). Conversely, 1.2-Li/ZrZn/MgO-SiO_2-1 sample presented a lower 1,3-BD yield and productivity, which is in line with its lower BET surface area, equal to 81 m²/g, compared to the surface area of 1.2-Na/ZrZn/MgO-SiO_2-1 and 1.2-K/ZrZn/MgO-SiO_2-1 samples, equal to 219 and 243 m²/g, respectively.

Finally, the effect of calcination step removal before Zr and Zn addition was investigated, entries 14-17. The removed calcination step is illustrated in the Figure S8 as *Calcination 1*. Regarding the ZrZn/MgO-SiO_2-1 system, a slight enhancement of ethene and diethyl ether selectivities was observed upon the removal of the calcination step (compare entry 1 and 14, Table 1), suggesting an increase in the acidity of the catalyst and/or an improvement in the access to active acid sites, since the BET surface area changed from 323 to 416 m²/g for the ZrZn/MgO-SiO_2-1 system prepared with and without the calcination step before Zr and Zn addition, respectively. For samples containing Na_2O, K_2O and Li_2O, the removal of calcination step was beneficial to 1,3-BD yield and productivity (compare entries 3 and 15 for Na_2O, entries 12 and 16 for K_2O, and 13 and 17 for Li_2O containing samples). As observed for the ZrZn/MgO-SiO_2-1 system, 1.2-K/ZrZn/MgO-SiO_2-1 and 1.2-Li/ZrZn/MgO-SiO_2-1 samples also presented an increase on surface area as a result of initial calcination step removal, Table S4.

These results suggest a clear relationship among 1,3-BD formation, acidic-basic concentration and its distribution on catalyst surface, since 1,3-BD yield and productivity were strongly correlated with catalyst surface area for samples containing alkali metals, Figure 9.

The effect of calcination steps removal was further investigated through ^{7}Li MAS NMR spectroscopy. Figure S9(a) shows spectra for samples 1.2-Li/ZrZn/MgO-SiO_2-1 and 1.2-Li/ZrZn/MgO-SiO_2-1 prepared with only 1 calcination step after ZrO_2 and ZnO addition. Even though a similar chemical shift was observed between the samples, the different lineshape, broader in the half width for the sample with higher number of calcination steps, Figure S9(b), and the different intensities of the spinning sideband distribution indicated a modification in the local environment of the lithium nuclei. Thus, the reduction of the calcination steps number, besides largely affecting surface area, in agreement with other studies,[44] also produces different structural ordering between samples.

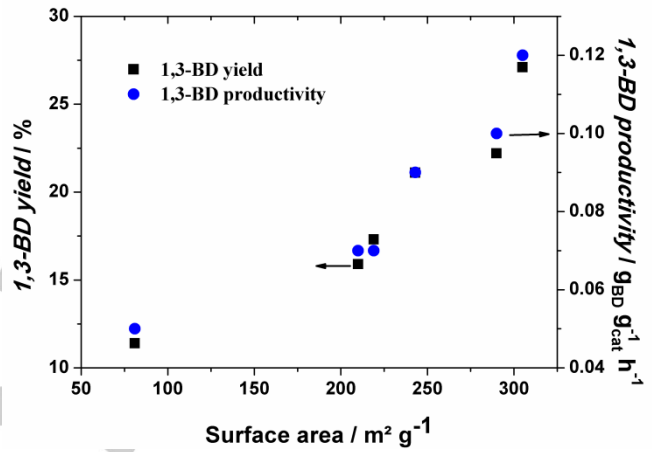

Figure 9. Relationship between surface area, 1,3-BD yield (left) and 1,3-BD productivity (right) for 1.2-Na/ZrZn/MgO-SiO_2-1, 1.2-K/ZrZn/MgO-SiO_2-1 and 1.2-Li/ZrZn/MgO-SiO_2-1 samples. Reactions performed as entries 3, 12, 13, 15-17, Table 1.

The catalyst 1.2-K/ZrZn/MgO-SiO_2-1 was further investigated regarding WHSV effects, entries 18-20, Table 1. A similar kinetic behaviour to the ZrZn/MgO-SiO_2-1 system at 325 ºC was observed, since higher contact times (obtained at lower WHSVs) were beneficial to 1,3-BD selectivity and yield.

Therefore, the acidity modification of the ZrZn/MgO-SiO_2-1 system prepared by co-precipitation, through the addition the alkali metals, specially using K_2O, seems to be a promising - and cheap - catalyst preparation method in order to maximize the 1,3-BD formation from ethanol conversion. Firstly, ethanol dehydration might be avoided, which is a thermodynamic requirement to achieve higher 1,3-BD yield. Besides, unconverted ethanol and acetaldehyde produced might be recycled in process, overcoming the lower ethanol conversion obtained with these systems.

Catalyst characterisation

The elemental dispersion of selected samples at specific locations on the catalyst particles was investigated through scanning electron microscopy with energy dispersive X-ray analysis. Table 2 shows average values determined. A general uniform distribution of Mg, Si, Zr, Zn and Na was observed.

Table 2. Elemental dispersion of catalyst samples in weight %.[a]

Sample	Mg	Si	Zr	Zn	Na
ZrZn/MgO-SiO_2-1	32.1 ± 0.5	59.6 ± 2.2	6.3 ± 2.0	1.4 ± 0.4	0.6 ± 0.2
0.8-Na/ZrZn/MgO-SiO_2-1	31.8 ± 1.0	56.7 ± 2.0	7.6 ± 2.5	1.7 ± 0.4	2.2 ± 0.2
1.2-Na/ZrZn/MgO-SiO_2-1	31.5 ± 0.9	55.8 ± 0.5	7.2 ± 0.3	1.9 ± 0.6	3.7 ± 0.5
2-Na/ZrZn/MgO-SiO_2-1	31.8 ± 0.4	56.7 ± 0.5	6.5 ± 0.7	1.9 ± 0.3	3.2 ± 0.1

[a] Values of Mg, Si, Zr, Zn and Na were normalised to 100 and represent a dispersion measure only.

However, a higher measurement scattering was observed for Zr, Zn and Na (compare standard deviations, Table 2), which may be due to a less uniform distribution of these compounds and/or related to a lower analysis sensitivity associated to the smaller concentration of these species. Moreover, the Na doping was confirmed by analyses, which highlight the different Na_2O content among samples. The residual amount of Na observed in the ZrZn/MgO-SiO_2-1 catalyst might be a result of an incomplete removal of Na during catalyst washing.

Element distribution of catalysts surface was further evaluated through EDX mapping analysis. Figure 10 shows element distribution for the 1.2-Na/ZrZn/MgO-SiO_2-1 catalyst, emphasising the homogeneous chemical distribution of elements.

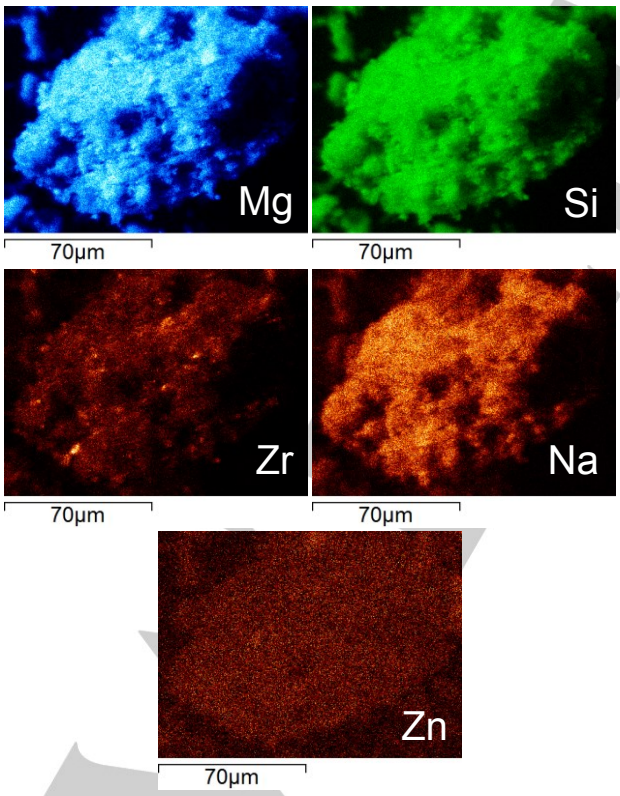

Figure 10. Elemental mapping of the 1.2-Na/ZrZn/MgO-SiO_2-1 catalyst.

Element distribution for samples 0.8-Na/ZrZn/MgO-SiO_2-1 and 2-Na/ZrZn/MgO-SiO_2-1 is shown in the Figures S10-S11. The dispersion homogeneity was further verified by an additional analysis using a higher magnification, Figure S12.

The metal loadings were confirmed by ICP-OES. Na loadings of 0.98 and 1.96, Zn loadings of 0.39 and 0.37, and Zr loadings of 1.13 and 1.07 % (wt.) were observed for samples 1.2-Na/ZrZn/MgO-SiO_2-1 and 2-Na/ZrZn/MgO-SiO_2-1, respectively.

Figure S13 shows the pXRD patterns for MgO-SiO_2 and the metal doped variants. Similar pXRD patterns were observed for K_2O and Li_2O containing samples, Figure S14, for the 1.2-Na/ZrZn/MgO-SiO_2-1 sample prepared with no calcination after Na doping, Figure S15, and for samples prepared with no calcination step before Zr and Zn addition, Figure S16. Thus, samples presented a common amorphous structure with the three broad peaks (at 25-30°, 33-39° and 58-62°) characteristic of magnesium silicate hydrates.[34,35]

The local environment of the silicon atoms on the catalyst surface was investigated through ^{29}Si MAS NMR spectroscopy, Figure S17. Figure S17(a) shows spectra for catalysts i) MgO-SiO_2-1, ii) ZrZn/MgO-SiO_2-1, iii) 0.8-Na/ZrZn/MgO-SiO_2-1, iv) 1.2-Na/ZrZn/MgO-SiO_2-1 and v) 2-Na/ZrZn/MgO-SiO_2-1. Spectra are in agreement with pXRD patterns, the two broad resonances with maxima around -87 and -95 ppm suggest the presence of -Mg-O-Si- linkages. Moreover, the lack of signal at -110 indicates the absence of silica in the catalyst structure, or the presence of an amount too small to be detected.[34] Similar signals with chemical shift between -85 and -89 ppm and between -92 and -99 ppm were already reported for magnesium silicate systems and they were attributed to Q^2 and Q^3 species, respectively, as $Si^*(OMg)(OSi)_2(OH)$ and $Si^*(OMg)(OSi)_3$.[2,34,36] ^{29}Si MAS spectra were confirmed by cross-polarization (CP) experiments, Figure S17(b). A shoulder at ca. -80 ppm was observed for all samples, which might be related to Q^1 species.

^{29}Si MAS spectra were fitted by a function containing two Gaussians in order to compute spectra areas and obtain the relative proportion of each silicon environment, the data being summarised in Table 3. Only subtle differences were

observed between the relative proportion of Q^2 and Q^3 species, which are probably due to the intrinsic experimental analysis fluctuation. This data indicates that catalytic results are not explained through the interaction of Na species with surface Brønsted acidic silanols moieties.

Table 3. Summary of ^{29}Si MAS NMR data. Numbers represent the relative proportion of each silicon environment.

Catalyst sample	Q^2 (-87 ppm)	Q^3 (-95 ppm)
i) MgO-SiO_2-1	21.9	78.1
ii) ZrZn/MgO-SiO_2-1	27.4	72.6
iii) 0.8-Na/ZrZn/MgO-SiO_2-1	28.6	71.4
iv) 1.2-Na/ZrZn/MgO-SiO_2-1	27.0	73.0
v) 2-Na/ZrZn/MgO-SiO_2-1	26.3	73.7

Furthermore, basicity features of catalyst samples were investigated through IR measurements from $CHCl_3$ adsorption,[45,46] Figure S18. Subtle differences in the $CHCl_3$ stretching intensities were observed among samples. A comparison with MgO suggested that samples containing higher alkali metal content (1.2 and 2 % (wt.)) may have a slightly higher basicity compared to the precursor MgO-SiO_2 and the ZrZn/MgO-SiO_2 system.

Therefore, the main effect of alkali metals doping may be related to their interaction with Lewis acid sites associated to ZrO_2 and ZnO species, as also suggested by NH_3-TPD experiments and IR measurements from NH_3 adsorption.

Conclusions

In this work, the effect of the Mg-to-Si molar ratio was investigated in the synthesis of magnesia silicate oxides prepared by co-precipitation for the ethanol to 1,3-butadiene conversion. Catalysts were used as support for ZrO_2 and ZnO and ethanol conversion was studied in a wide range of WHSVs using two reaction temperatures. ^{29}Si MAS NMR data suggested that the co-precipitation method was more efficient in the formation of Mg-O-Si linkages, compared to the traditional wet-kneading. The Mg:Si molar ratio equal to 1 was more suitable to 1,3-BD formation, while higher Mg:Si molar ratios produced more acetaldehyde. High 1,3-BD productivities (in $g_{BD}/g_{cat}\cdot h$) were obtained with the ZrZn/MgO-SiO_2-1 system, results that might be associated to the homogeneity of the catalyst properties. Catalytic results supported the usual kinetic route of ethanol to 1,3-BD conversion involving acetaldehyde condensation. The catalyst acidity was modified through the addition of alkali metals (Me = Na, Li and K) to the final materials. This process resulted in a decrease of the fraction of ethanol dehydrated, boosting 1,3-BD selectivity. A positive linear relation was obtained for the combined 1,3-BD and acetaldehyde selectivities as a function of the catalyst Na content. Further catalyst optimization was performed through the reduction of calcination steps in the catalyst preparation, resulting in higher surface areas, 1,3-BD yields and productivities. In particular, a strong correlation between surface area, 1,3-BD yield and productivity was observed for 1.2-Me/ZrZn/MgO-SiO2-1 samples. Thus, efforts should be dedicated in order to increase surface area of these systems, keeping the acid-basic distribution constant. The best catalytic results were obtained with the 1.2-K/ZrZn/MgO-SiO_2-1 material, achieving 72 mol% for the combined selectivity of 1,3-BD and acetaldehyde, at reasonable 1,3-BD yield and productivity level. Therefore, since unconverted ethanol and acetaldehyde may easily be recycled in the process, the *x*-K/ZrZn/MgO-SiO_2-1 system prepared by co-precipitation is a promising material that deserves more investigation in order to maximize 1,3-BD production. Catalyst acidity modification was further confirmed by NH_3-TPD and IR measurements from NH_3 adsorption, but ^{29}Si MAS NMR data indicated that the role of the alkali metal in the catalyst structure was not related to its interaction with Brønsted acidic silanols moieties. Since IR measurements from $CHCl_3$ adsorption indicated only subtle differences between catalysts basicity, the main effect of alkali metal doping should be associated to a selective deactivation of Lewis acid sites related to ZrO_2 and ZnO.

Experimental Section

Catalyst preparation

In a typical synthesis, catalysts at the Mg:Si molar ratio equal to 25:75, 50:50, 75:25 and 95:5 were prepared by co-precipitation. For the 50:50 material, 9.01 g of SiO_2 (Sigma-Aldrich (SA), 99.8 %) was dissolved in 100 mL of 1.2 M NaOH solution (SA, 99 %). The mixture was heated between 60 and 80 °C under vigorous stirring until complete SiO_2 dissolution, the solution was cooled and 42.4 g of Na_2CO_3 (SA, 99.9 %) added. A $Mg(NO_3)_2\cdot 6H_2O$ solution (SA, 99 %) was added drop-wise into this mixture whilst stirring at 25 °C (38.85 g of $Mg(NO_3)_2\cdot 6H_2O$ in 200 mL). The pH was maintained at 10.5 by adding appropriate quantities of 1.2 M NaOH solution and, at the end of the process, the solution volume was adjusted to 600 mL with deionized water. The resultant mixture was stirred for 2 h before ageing for 22 h at 25 °C. Finally, the mixture was filtered and washed with 7.5 L of hot water. The precipitate was dried in static air at 80 °C for 24 h before grinding. Materials were calcined in air at 500 °C for 4 h, using a heating rate of 5 °C/min.

In order to produce materials with 1.5 %, 0.5 % weight of Zr(IV) and Zn(II), respectively, 0.57 g of $ZrO(NO_3)_2\cdot H_2O$ (SA, 99 %) and 0.24 g of $Zn(NO_3)_2\cdot 6H_2O$ (SA, 98 %) were dissolved in 50 mL of water, and the solution was added to 10 g of the MgO-SiO_2 system. This was stirred until the mixture was completely dry. Finally, the solid was calcined in air at 500 °C for 5 h. For the Na doping, the appropriate volume of 1.2 M NaOH solution was added to the final catalyst drop-wise. The mixture was kept under stirring during 1 h at 25 °C before drying at 80 °C for 5.5 h and finally calcined at the same previous condition. KOH (SA, 90 %) and $LiOH\cdot H_2O$ (Alfa Aesar, 99 %) were used instead of NaOH for comparison. The catalyst preparation procedure is illustrated in the Scheme 1 in the Support

ACCEPTED

Information (SI). Samples were labelled as *y-Me*/ZrZn/MgO-SiO_2-*x*, where *y* denotes the content of the alkali metal *Me* in weight % and *x* represents the Mg:Si molar ratio.

Catalyst Characterisation

SEM images and SEM/EDX mapping were carried out on a JEOL6480LV at 5-25 kV. Energy-dispersive X-ray spectroscopy (EDX) was carried out *in-situ* during SEM analysis. At least 5 different spots were selected throughout the images, to evaluate the homogeneity of elements within catalyst particles. Measurements of static adsorption of N_2 at -196 °C were obtained using a Micromeritics 3Flex instrument. Samples were degassed at 150 °C under vacuum for 2 h prior to analysis. Powder X-ray diffraction (PXRD) was performed on a BRUKER D8-Advance diffractometer using CuKα (λ = 1.5406 Å) radiation. Intensities were measured with a 0.02° step size and a measuring time of 0.3 s per point. ^{29}Si solid-state MAS NMR was performed using a Varian VNMRS 400 MHz spectrometer, operating at a resonance frequency of 79.44 MHz with a spinning rate of 6 kHz. 1,000 scans were accumulated with a recycle time of 60 s, the pulse length being 4.5 µs. The ^{29}Si{^{1}H} CP MAS NMR spectra were recorded on the same spectrometer. 4,000 scans were accumulated with a recycle time of 1 s. The CP contact time was 3.0 ms. The ^{29}Si chemical shifts are referenced to tetramethylsilane. Acidity of samples were determined by temperature programmed desorption of ammonia (NH_3-TPD) in a Setsys Evolution TGA Setaram system coupled with an in-line mass spectrometer, OmniStar™ Pfeiffer Vacuum Quadrupole, for measurement of the outgas composition. The release of ammonia (m/z=15) was monitored. The signal m/z equal to 15 was used in order to avoid interference by the fragmentation of water molecules. Samples were exposed to NH_3 for 48 h at room temperature before TPD experiment. Pure argon, 100 mL/min, was used as sweep gas. Before starting the analysis, the analytical chamber was purged from ambient air using argon flow at 200 mL/min for 40 min. The NH_3-TPD analyses were started by heating the sample at 10 °C/min from room temperature to 700 °C and maintaining that temperature for 0.5 h, under argon. In situ IR spectra were recorded on a PerkinElmer Frontier spectrometer. Measurements were performed accumulating 15-30 scans at a resolution of 4 cm^{-1}. $CHCl_3$ was used as a molecular probe for basicity evaluation.[45] Samples were exposed to $CHCl_3$ at 20 ºC. MgO (Sigma-Aldrich) was evaluated for comparison.

Catalytic reactions

The catalytic tests were carried out in a flow quartz packed-bed reactor at atmospheric pressure. Argon was used as carrier gas (8 ml/min). The ethanol weight hourly space velocity (WHSV) was varied within 0.3-2.4 h^{-1} through the modification of ethanol flow rate, keeping catalyst mass and carrier gas flow rate fixed. The WHSV range investigated corresponded to ethanol molar fractions between 0.41 and 0.85. The contact time (calculated as the ratio between the catalyst volume and the total gas flow at the reaction temperature) ranged from 1.3 to 5.5 sec. Reaction temperature was within 325-375 °C. The exhaust gases were analysed after 3 h of time on stream (TOS) via GC-MS on an Agilent 7890A instrument with a HP-PLOT/Q, 30 m long 0.53 mm diameter column equipped with FID/MS detectors. The GC was calibrated as detailed elsewhere.[13] Carbon balances were typically better than 80 %. Carbon balances and reaction conditions are summarized in the Table S5.

Ethanol conversion (X), selectivity (S) and yield were computed as Equation 1, 2 and 3, respectively, where $N_{EtOH,in}$ and $N_{EtOH,out}$ represent the number of mols of ethanol that were added and collected, respectively, N_i denotes the number of mols of the product *i*, *NP* is the total number of products and *r* is the ratio between the number of carbons of the product *i* and of ethanol. For 1,3-BD, for instance, *r* is equal to 2.

$$\boldsymbol{X}(\%) = \frac{\mathbf{N_{EtOH,in} - N_{EtOH,out}}}{\mathbf{N_{EtOH,in}}} \cdot \mathbf{100} \quad (1)$$

$$\boldsymbol{S_i}(\%) = \frac{\mathbf{N_i}}{\sum_{i=1}^{NP} \mathbf{N_i}} \cdot \mathbf{100} \quad (2)$$

$$\boldsymbol{yield}(\%) = \frac{\mathbf{r \cdot N_i}}{\mathbf{N_{EtOH,in}}} \cdot \mathbf{100} \quad (3)$$

Acknowledgements

The authors thank CNPq (Conselho Nacional de Desenvolvimento Científico e Tecnológico, Brazil) for supporting this research and providing scholarships. We wish to thank the EPSRC Solid-state NMR facility in Durham (Dr David Apperley). We thank the Universities of Bath and Cardiff for involvement in the GW4 partnership.

Keywords: green chemistry • heterogeneous catalysis • ethanol • 1,3-butadiene • silica-magnesia catalyst

[1] D. Cespi, F. Passarini, I. Vassura, F. Cavani, *Green Chem.* **2015**, *18*, 1625-1638.
[2] W. Janssens, E. V. Makshina, P. Vanelderen, F. De Clippel, K. Houthoofd, S. Kerkhofs, J. A. Martens, P.A. Jacobs, B. F. Sels, *ChemSusChem* **2015**, *8*, 994-1008.
[3] W. C. White, *Chem. Biol. Interact*. **2007**, *166*, 10-14.
[4] G. Odian. *Principles of polymerization*, fourth ed., John Wiley & Sons, Inc., New York, **2004**, pp. 529-533.
[5] E. V. Makshina, M. Dusselier, W. Janssens, J. Degrève, P. A. Jacobs, B. F. Sels, *Chem. Soc. Rev*. ***2014***, *43*, 7917-7953.
[6] P. C. A. Bruijnincx, B. M. Weckhuysen, *Angew. Chem. Int. Ed*. **2013**, *52*, 11980-11987.
[7] C. Angelici, B. M. Weckhuysen, P. C. A. Bruijnincx, *ChemSusChem* **2013**, *6*, 1595-1614.
[8] J. A. Posada, A. D. Patel, A. Roes, K. Blok, A. P. C. Faaij and M. K. Patel, *Bioresour. Technol.* **2013**, *135*, 490-499.
[9] *http://www.afdc.energy.gov/data/10331,* ***2016***.
[10] H. Niiyama, S. Morii, E. Echigoya, *Bull. Chem. Soc. Jpn*. **1972**, *45*, 655-659.
[11] S. Kvisle, A. Aguero, R.P.A. Sneeden, *Appl. Catal.* **1988**, *43*, 117-131.
[12] M. D. Jones, C. G. Keir, C. Di Iulio, R. A. M. Robertson, C. V. Williams, D. C. Apperley, *Catal. Sci. Technol*. **2011**, *1*, 267-272.
[13] E. V. Makshina, W. Janssens, B. F. Sels, P. A. Jacobs, *Catal. Today.* **2012**, *198*, 338-344.
[14] V. L. Sushkevich, I. I. Ivanova, V. V Ordomsky, E. Taarning, *ChemSusChem* **2014**, *7*, 2527-2536.
[15] M. Gao, Z. Liu, M. Zhang, L. Tong, *Catal. Lett.*, 2014, **144**, 2071-2079.
[16] V. L. Sushkevich, I. I. Ivanova, E. Taarning, *Green Chem.* **2015**, *17*, 2552-2559.
[17] W. M. Quattlebaum, W. J. Toussaint and J. T. Dunn, *J. Am. Chem. Soc.* **1947**, *69*, 593.
[18] J. V. Ochoa, C. Bandinelli, O. Vozniuk, *Green Chem.* **2015**, *18*, 1653-1663.
[19] A. Chieregato, J. Velasquez Ochoa, C. Bandinelli, G. Fornasari, F. Cavani, M. Mella, *ChemSusChem* **2015**, *8*, 377-388.

WILEY-VCH

[20] J. I. Di Cosimo, V. K. Diez, M. Xu, E. Iglesia, C.R. Apesteguía, *J. Catal.* **1998**, *178*, 499-510.
[21] V. V. Ordomsky, V. L. Sushkevich, I. I. Ivanova, *J. Mol. Catal. A: Chem.* **2010**, *333*, 85-93.
[22] C. Angelici, M. E. Z. Velthoen, B. M. Weckhuysen, P. C. A. Bruijnincx, *ChemSusChem* **2014**, *7*, 2505-2515.
[23] M. Lewandowski, G. S. Babu, M. Vezzoli, M. D. Jones, R. E. Owen, D. Mattia, P. Plucinski, E. Mikolajska, A. Ochenduszko, D. C. Apperley, *Catal. Commun.* **2014**, *49*, 25-28.
[24] Z. Han, X. Li, M. Zhang, Z. Liu, M. Gao, *RSC Adv.* **2015**, *5*, 103982-103988.
[25] M. León, E. Díaz, S. Ordóñez, *Catal. Today* **2011**, *164*, 436-442.
[26] M. León, E. Díaz, A. Vega, S. Ordóñez, A. Auroux, *Appl. Catal., B* **2011**, *102*, 590-599.
[27] C. Angelici, M. E. Z. Velthoen, B. M. Weckhuysen and P. C. A. Bruijnincx, *Catal. Sci. Technol.* **2015**, *5*, 2869-2879.
[28] O. V. Larina, P. I. Kyriienko and S. O. Soloviev, *Catal. Lett.* **2015**, *145*, 1162-1168.
[29] Y. Sekiguchi, S. Akiyama, W. Urakawa, T. Koyama, A. Miyaji, K. Motokura and T. Baba, *Catal. Commun.* **2015**, *68*, 20-24.
[30] R. A. L. Baylon, J. Sun and Y. Wang, *Catal. Today* **2016**, *259*, 446-452.
[31] T. D. Baerdemaeker, M. Feyen, U. Müller, B. Yilmaz, F.-S. Xiao, W. Zhang, T. Yokoi, X. Bao, H. Gies, D. E. De Vos, *ACS Catal*. 2015, *5*, 3392-3397.
[32] A. Klein, K. Keisers, R. Palkovits, *Appl. Catal., A* **2016**, *514*, *192-202.*
[33] H.-J. Chae, T.-W. Kim, Y.-K. Moon, H.-K. Kim, K.-E. Jeong, C.-U. Kim, S.-Y. Jeong, *Appl. Catal., A* **2014**, *150-151*, 596-604.
[34] D. R. M. Brew and F.P. Glasser, *Cem. Concr. Res.* **2005**, *35*, 85-98.
[35] Z. Li, T. Zhang, J. Hu, Y. Tang, Y. Niu, J. Wei and Q. Yu, *Constr. Build. Mater.* **2014**, *61*, 252-259.
[36] J. S. Hartman and R. L. Millard, *Phys. Chem. Minerals* **1990**, *17*, 1-8.
[37] C. Perego and S. Peratello, *Catal. Today **1999**, 52*, 133-145.
[38] H. Knözinger and R. Köhne, *J. Catal*. **1966**, *5*, 264-270.
[39] J. R. Jain and C. N. Pillai, *J. Catal.* **1967**, *9*, 322-330.
[40] B. Shi and B. H. Davis, *J. Catal.* **1995**, *157*, 359-367.
[41] H. Arai, J.-I. Take, Y. Saito and Y. Yoneda , *J. Catal.* **1967**, *9*, 146-153.
[42] H. Knözinger, H. Bühl and K. Kochloefl, *J. Catal.* **1972**, *24*, 57-68.
[43] V. Gruver, A. Sun and J. J. Fripiat, *Catal. Lett.* **1995**, *34*, 359-364.
[44] S. Da Ros, E. Barbosa-Coutinho, M. Schwaab, V. Calsavara and N. R. C. Fernandes-Machado, *Mater. Charact.* **2013**, *80*, 50-61.
[45] M. Tamura, K.-I. Shimizu, A. Satsuma, *Appl. Catal., A* **2012**, *433-434*, 135-145.
[46] S. Huber, H. Knözinger, *J. Mol. Catal. A: Chem.* **1999**, *141*, 117-127.

WILEY-VCH

FULL PAPER

Ethanol to 1,3-butadiene: The catalyst acidity role of ZrZn containing silica magnesia oxides prepared by co-precipitation method has been investigated. Catalyst acidity control is the key step in order to increase butadiene selectivity.

S. Da Ros, M. D. Jones, D. Mattia, J. C. Pinto, M. Schwaab, F. B. Noronha, S. A. Kondrat, T. C. Clarke, S. H. Taylor*

Page 1. – Page 12.

Title Ethanol to 1,3-butadiene conversion using ZrZn-containing $MgO\text{-}SiO_2$ systems prepared by co-precipitation: effect of catalyst acidity modification

Key words: Ethanol, butadiene, heterogeneous catalysis

WILEY-VCH